SPACE RESEARCH COORDINATION CENTER

EXCITATION OF Na D-LINE RADIATION IN COLLISIONS OF SODIUM ATOMS WITH INTERNALLY EXCITED H_2, D_2 AND N_2^*

BY

H. F. KRAUSE, J. FRICKE, AND W. L. FITE

SRCC REPORT NO. 167

UNIVERSITY OF PITTSBURGH

PITTSBURGH, PENNSYLVANIA

FEBRUARY 1972

The Space Research Coordination Center, established in May, 1963, has the following functions: (1) it administers predoctoral and postdoctoral fellowships in space-related science and engineering programs; (2) it makes available, on application and after review, allocations to assist new faculty members in the Division of the Natural Sciences and the School of Engineering to initiate research programs or to permit established faculty members to do preliminary; work on research ideas of a novel character; (3) in the Division of the Natural Sciences it makes an annual allocation of funds to the Interdisciplinary Laboratory for Atmospheric and Space Sciences; (4) in the School of Engineering it makes a similar allocation of funds to the Department of Metallurgical and Materials Engineering and to the program in Engineering Systems Management of the Department of Industrial Engineering; and (5) in concert with the University's Knowledge Availability Systems Center, it seeks to assist in the orderly transfer of new space-generated knowledge in industrial application. The Center also issues periodic reports of space-oriented research and a comprehensive annual report.

The Center is supported by an Institutional Grant (NsG-416) from the National Aeronautics and Space Administration, strongly supplemented by grants from the A. W. Mellon Educational and Charitable Trust, the Maurice Falk Medical Fund, the Richard King Mellon Foundation and the Sarah Mellon Scaife Foundation. Much of the work described in SRCC reports is financed by other grants, made to individual faculty members.

Excitation of Na D-Line Radiation in Collisions of Sodium Atoms with Internally Excited H_2, D_2 and N_2*

H. F. Krause†, J. Fricke‡, and W. L. Fite
Department of Physics
University of Pittsburgh
Pittsburgh, Pennsylvania 15213

Abstract

Excitation of D-line radiation in collisions of Na atoms with vibrationally excited N_2, H_2 and D_2 has been studied in two modulated crossed beam experiments. In both experiments, the vibrational excitation of the molecules was provided by heating the molecular beam source to temperatures in the range of 2000 to 3000°K, which was assumed to give populations according to the Boltzmann expression. In the first experiment, a total rate coefficient was measured as a function of molecular beam temperature, with absolute calibration of the photon detector being made using the black body radiation from the heated molecular beam source. Since heating affects both the internal energy and the collisional kinetic energy, the first experiment could not determine the relative contributions of internal energy transfer *vs.* collisional excitation. The second experiment achieved partial separation of internal *vs.* kinetic energy transfer effects by using a velocity-selected molecular beam.

---

*This research was supported in part by the National Aeronautics and Space Administration under Grant No. NGL 39-011-013 and the Advanced Research Projects Agency through the U. S. Army Research Office - Durham.

†Present Address: Oak Ridge National Laboratory, Oak Ridge, Tennessee, 37830

‡Present Address: Physik Department, Technische Universitat, Munchen, Germany.

Using two simple models for the kinetic energy dependence of the transfer cross section for a given change in vibrational quantum number, the data from both experiments were used to determine parameters in the models. Evidently the most probable situation is that most of the Na excitation energy comes from internal vibrational energy, with the remainder coming from kinetic energy. The paper discusses the consequences of the detailed results with respect to the excitation of sodium radiation in aurorae.

I. INTRODUCTION

It has been known for many years that the resonance radiation of sodium atoms is efficiently quenched in the presence of molecular gases such as H_2, D_2 and N_2. The high quenching efficiency for these molecules, compared to the inefficient quenching by atomic gases, was usually attributed to efficient energy transfer involving internal molecular states. Although effective quenching cross sections for molecular gases had been studied extensively in a variety of environments[1], the electronic-internal energy transfer mechanism was speculative because neither reaction product's kinetic energy had been determined nor their vibrationally excited states identified.

The first several experiments appearing to confirm that the electronic-vibrational transfer hypothesis might be correct, at least for the case of sodium, were some investigations of the inverse process for N_2 carried out in shock tubes.[2] The slow rise of the sodium-line reversal temperature behind the shock front suggested to Clouston, Gaydon, and Glass[3] that the excitation of sodium atoms was due to vibrationally excited N_2 molecules. Stronger evidence that this suggestion was correct subsequently came from Haydon and Hurle[4] and Hurle[5] who showed that, in shock-heated N_2 containing Na, the Na excitation temperature follows the relaxing vibrational temperature of N_2 rather than the N_2 translational temperature. Hurle[5] concluded that the transfer of excitation energy from N_2 vibrational modes proceeds with much higher probability ($\sigma > 3 \times 10^{-16} cm^2$) than the transfer from rotational or kinetic energy modes.

This result appeared to be confirmed in a sodium excitation experiment by Starr[6], where vibrationally excited N_2 was produced in the

afterglow of a microwave discharge in flowing N_2. In this experiment, all strong sodium lines between 3100-6100Å were examined. Since a number of sodium levels were excited similarly as the $Na(3^2P)$, Starr additionally concluded that a close match between the vibrational and electronic levels is not requisite for the process to occur.

Around the time that Hurle and Starr offered evidence supporting the efficient interconversion of electronic and vibrational energy between Na and N_2, Derblom[7] positively identified the yellow emission observed in Type B aurora as due to Na D-line emission. While a number of mechanisms had been postulated to explain its origin, Hunten[8] proposed that the excitation of Na atoms arose through the transfer of N_2 vibrational energy.

Hunten noted that in auroras there are electrons with sufficient energy to excite the Na atoms directly, but there is a large cross section for these electrons to excite N_2 vibrationally in states up to $v = 8$. Competition for the fast electrons would most certainly be won by the much more numerous N_2 molecules. Further noting that the energy of the $v = 8$ state of N_2 is only about 0.1 eV greater than the energy required to excite D-line radiation, Hunten proposed that N_2 takes the energy from the electrons, stores it in the $v = 8$ state, and then transmits it on to the Na atoms. Whether this proposal was tenable depended on knowledge of the sodium D-line excitation cross section for the near resonant vibrational states and only the lower cross section limit determined by Hurle[5] was available.

In an effort to provide more specific cross sectional information for collisional Na D-line excitation mechanisms, a series of crossed beam excitation experiments were initiated at this laboratory using the species N_2, H_2 and D_2.

In these excitation experiments, the molecular species issued from the furnace source operating in the temperature range 2000-3000°K, while the sodium atoms effused from a 650° source. The D-line radiation emitted from the beam intersection region was observed. The basic experiments for these species were designed to determine the excitation rate constant as a function of the molecular beam temperature. The later velocity-selected molecular beam experiments were directed toward a more detailed understanding of the reaction mechanism, i.e., deduction of the participating vibrational states and their cross sections for excitation transfer.

The basic experiment for the N_2 - Na system performed by Mentall, Krause, and Fite has been previously reported[9] along with a preliminary analysis. The present report describes the extension of the previous experiment to include H_2 and D_2 molecules, experiments using velocity selection and an analysis of both.

II. PRINCIPLES OF THE EXPERIMENT

Excitation of the first resonance doublet of Na in collisions with the diatomic molecules H_2, D_2 and N_2 is represented by Eq. (1) when the reacting species originate from sources operating at thermal energies.

$$A_2(X\ ^1\Sigma_g^+, \varepsilon) + Na(3^2S) + E \rightarrow A_2(X\ ^1\Sigma_g^+, \varepsilon') + Na(3^2P) + E' \qquad (1)$$

The molecular internal energy before and after collision, represented by ε and ε', is due to vibration and rotation. Since the atom receives electronic energy, $E_o = 2.10$ eV, during the collision, conservation of energy implies that this energy must come from the change in internal energy, $\Delta\varepsilon$, and kinetic energy, ΔE, before and after collision.

$$\Delta\varepsilon + \Delta E = E_o \qquad (2)$$

The experimental arrangement which utilized beams crossed at 90^o is shown schematically in Fig. 1. The diatomic gas was excited thermally in a tungsten furnace operating at temperature, T_1, between 2000 and 3000^oK. Since each molecule made on the average approximately 10^3 collisions with the walls before escaping into the beam, it was assumed that the gas reached equilibrium with the furnace walls and the degree of excitation of internal energy states was given by the Boltzmann distribution. Since vibrational excitation in N_2, D_2 and H_2 cannot be lost through radiation, the beam's vibrational population does not differ from that in the furnace. The sodium atom beam had a kinetic temperature, $T_2 = 650^oK$.

Sodium D-line photons produced by the interaction of the molecular and Na beams were collected by a lens and detected by a cooled

photomultiplier which views the interaction region. Wavelength discrimination was achieved by the use of a 20Å band-pass interference filter. This bandwidth still admitted a large signal due to the hot tungsten furnace light reflected from the blackened walls of the experimental vacuum chamber. To distinguish this reflected radiation from radiation arising from the colliding beams, the sodium beam was modulated at 1440 Hz by a rotating chopper wheel. By feeding the photomultiplier signals to lock-in amplifier circuitry, the desired signal is identified, since it occurs at the sodium beam modulation frequency and in specified phase.

A. Basic Configuration

In the "basic configuration", both beams had their full Maxwellian velocity distributions, and the sodium beam was always exposed to the light from the furnace. Resonant scattering of the light by the modulated sodium beam gave rise to a modulated photon signal, which could be distinguished from the collision-produced signal by noting changes in signal as the gas admitted to the furnace was turned off and on. This resonantly scattered photon signal was used to advantage, since it provided absolute calibration for measurement of the collisional reaction rate coefficient.

In the present experiment, collimation was made sufficiently precise that virtually all of the light intersecting the Na beam came only from the aperture in the furnace. To very good approximation, the light spectrum is given by Planck's black-body radiation formula. It is straightforward to derive[10] that the resonantly scattered signal S_s is given by

$$S_s = \frac{3}{4\pi}\frac{V}{L^2} A_1 \Omega H n_2 \Gamma e^{-E_o/kT_1} \qquad (3)$$

where V is the volume of intersection of the light and Na beams, L is the distance from the furnace to the Na beam, A_1 is the area of the furnace aperture, Ω, is the solid angle subtended to the photon detector, H is the detection efficiency, n_2 is the Na atom density, Γ is the inverse radiative lifetime for the Na(^{3}P) states, E_o is the D-line photon energy, and T_1 is the temperature of the furnace. In deriving this formula the Planck black-body formula has been simplified for the limit $E_o/kT_1 \gg 1$, and the anisotropy[11] of the scattered radiation (about 5%) has been neglected.

The photon signal, S_r, arising from collisions of the molecules with the Na atoms is given by

$$S_r = V\Omega H\, n_1 n_2 k_r = Ck_r, \qquad (4)$$

where V, Ω, H, and n_2 have the same meanings as before, n_1 is the total number density in the Maxwellian molecular beam, and k_r is the reaction rate coefficient. Dividing Eq. (3) by Eq. (4), the rate coefficient is given by

$$k_r = \frac{3}{4\pi}\frac{\Gamma}{n_1}\frac{A_1}{L^2}\frac{S_r}{S_s}. \qquad (5)$$

By comparing the resonantly scattered photon signal with the collision-produced signals, it is unnecessary to independently determine the interaction volume, the Na beam intensity and the characteristics of the photon detection system. Γ is well known and the geometrical terms A_1 and L are easily determined. The number density in the molecular beam, n_1, is determined by noting the pressure increase, ΔP_3, in the

main vacuum chamber when the beam is admitted, converting this reading into the number density increase, Δn_3, and determining the total beam current, I_1, from the expression

$$I_1 = \Delta n_3 \cdot S_3, \tag{6}$$

where S_3 is the pumping speed of the pumps on the main vacuum chamber. (The pumping speed was independently measured by determining the vacuum chamber time constant, τ, and the volume, V_3, of the chamber, from which $S_3 = V_3/\tau$). The number density, n_1, is then given by

$$n_1 = \frac{I_1}{A_2 \bar{u}_1}, \tag{7}$$

where A_2 is the cross-sectional area of the molecular beam at the point of intersection with the Na beam (determinable from collimation geometry), and $\bar{u}_1 = ((8kT_1/\pi m_1)^{1/2})$ is the molecular mean speed averaged over the Maxwellian distribution based on number density.

In practice, the matter of comparing the resonantly scattered photon signal with the collision-produced signal is more complex because of the very large intensity of the scattered light signal compared to that of the collision-produced signal. The furnace light capable of exciting the Na D-lines must be attenuated by about three orders of magnitude in order to observe the signals from the collisions. This attenuation was accomplished by inserting an absorption cell containing sodium vapor along the molecular beam path (Fig. 1).

The sodium beam was collimated and has a very narrow spread of velocity components at right angles to it, i.e., along the direction from which the photons come, so that the Doppler width for the beam is extremely narrow. The Doppler width for the gas in the absorption cell,

on the other hand, was broad because of the fully random motion of the atoms in the cell, which absorbes light over a broad band centered on the narrow band for photon scattering by the beam. The high value of the effective photon absorption cross section of the cell ($\sim 10^{-11}$ cm^2 peak for the 600°K Na) compared to the atomic cross sections ($\lesssim 10^{-14}$ cm^2) implies that attenuation of the light by three orders of magnitude can be accomplished, while attenuating the molecular beam by less than 1%. The fact that sodium atoms effuse from the absorption cell into the region viewed by the photon detector, where they can resonantly scatter furnace light and add to the scattered signal from the beam, is not a problem. These additional atoms give rise to a dc signal, which is not detected by the ac detection circuitry.

The quantity under measurement in this experiment, k_r, is the integral of the rate constants for each of the internally excited states in the molecular beam. Defining $\sigma_r(\varepsilon,u)$ as the cross section for exciting the sodium for states of internal energy, ε, and the relative velocity, w, and calling $g(\varepsilon)$ the statistical weight density of states with internal energy, ε, it is convenient to define the quantity

$$\bar{\sigma}(w, T_1) = \frac{\int_0^\infty \sigma_r(\varepsilon,w) g(\varepsilon) e^{-\varepsilon/kT_1}\, d\varepsilon}{\int_0^\infty g(\varepsilon)\, e^{-\varepsilon/kT_1}\, d\varepsilon} \tag{8}$$

which is the cross section as a function of relative velocity, averaged over all molecular internal energy states populated at the temperature T_1.

The rate coefficient is then given by

$$k_r(T_1) = \int_0^\infty \int_0^\infty \bar{\sigma}(w,T_1) w f_1(u_1) f_2(u_2) du_1 du_2, \tag{9}$$

where $w = |\vec{u}_1 - \vec{u}_2|$ and

$$f_i(u_i) = \frac{4}{\sqrt{\pi}} (\alpha_i)^{3/2} u_i^2 e^{-\alpha_i u_i^2}, \qquad \alpha_i = \frac{m_i}{2kT_i} \qquad (10)$$

and m_1 and m_2 are the masses of the molecule and the Na atoms and T_2 is the sodium beam source temperature.

For beams crossing at right angles, Eq. (9) can be integrated once to yield

$$k_r = \frac{2(\alpha_1\alpha_2)^{3/2}}{\delta} \int_0^\infty \bar{\sigma}(w,T_1) w^4 I_1(\delta w^2) e^{-\gamma w^2} dw, \qquad (11)$$

where $\gamma = (\alpha_2 + \alpha_1)/2$, $\delta = (\alpha_2 - \alpha_1)/2$, and I_1 is the first order modified Bessel's function of the first kind.

The relative velocity distribution contained in Eq. (11) is somewhat similar to a Maxwellian distribution, but with a "temperature", based on mean relative speed, of only about half T_1 in the case of N_2 + Na, but closer to T_1 in the H_2 + Na and D_2 + Na cases. Thus the crossed beam configuration in an experiment of this kind presents a situation where the internal energy temperature can almost double the kinetic "temperature".

The rate coefficient, k_r, is a function of both T_1 and T_2, although in the present experiment T_2 is held constant at about 650°K. Variation of the temperature T_1 changes both the population of internal energy states and the distribution of kinetic energies of collision, and gives the first information about the roles of the internal energy states.

In order to cause the Na excitation it is necessary to provide 2.10 eV (E_o) from either internal or kinetic energy, and this energy is

provided from the temperature, T_1. The rate coefficient, k_r, is expected to be strongly temperature dependent, similar to $k_r \sim e^{-E_o/kT_1}$. A new quantity

$$\eta(T_1) = k_r(T_1)e^{E_o/kT_1}, \tag{12}$$

is defined, which can be thought of loosely as the rate coefficient for only those molecules which have sufficient energy to cause the excitation.

B. Velocity-Selected Configuration

Knowledge of the variation of the rate constants, k_r and η, with temperature is not sufficient to isolate the mechanism for reaction unambiguously; the observed temperature dependence may be ascribed to the transfer of pure internal energy and/or internal energy combining with varying amounts of kinetic energy, to provide the required reaction endoenergicity. The interpretational ambiguity, which results from the fact that the kinetic and internal energy distribution functions are characterized by the same parameter, T_1, and are changing simultaneously, can only be resolved by obtaining different experimental information. The interpretation can be clarified if the reactive signals are studied by varying the two distribution functions independently of each other.

The velocity distribution of molecules having a fixed internal energy distribution can be varied by inserting a velocity selector into the molecular beam. Since such a device can be made to pass excited molecules with little velocity dispersion over a broad range of transmitted speeds, the reaction can be studied as a function of molecular speed for each molecular furnace temperature. Appropriately, the velocity selector, which is of the rotating slotted disc type, simultaneously removes black-body tungsten furnace photons from the beam since the velocity of light falls outside of the selector transmission function at the molecular speeds of interest. For this reason, the sodium vapor absorption cell is not a required piece of apparatus when the velocity selector is inserted.

As in the basic configuration, the signal produced in the velocity-selected configuration can be described by a rate equation identical with

Eq. (4), with the rate coefficient being given by Eq. (9). The only difference is, that while $f_2(u_2)$ is the Maxwellian distribution given by Eq. (10), the distribution function, $f_1(u_1)$ must be altered by being multiplied by the transmission function of the velocity selector. The rate coefficient is therefore described by

$$k_r'(T_1,V_o) = \int_0^\infty \int_0^\infty \bar{\sigma}(wT_1)wf_1(u_1)B(V_0,u_1)f_2(u_2)du_1du_2, \qquad (13)$$

where $B(V_0,u_1)$, the transmission function, is the fraction of molecules having the speed, u_1, that are transmitted when the velocity selector is set to have maximum transmission for molecules with the speed V_o. A first integration of Eq. (13) cannot be done in closed form as was done to obtain Eq. (11), but was evaluated numerically using a computer. Final integration of both Eqs. (11) and (13) was done numerically.

III. APPARATUS

A. Vacuum System

The experiments were performed in a three-chamber differentially-pumped vacuum system. The molecular source was located in chamber one, while chamber three contained the remaining items necessary for the experiments. All vacuum system surfaces located in the experimental region were blackened with Aqua Dag in order to minimize stray furnace light that might easily be reflected into the optical system and cause excessive photomultiplier shot noise.

The first collimation aperture was kept smaller than the tungsten furnace aperture in order to allow only the photons from the aperture, and not the tungsten furnace wall, to travel axially from chamber one. The second collimating aperture was adjusted simultaneously to collimate the molecular beam and photons so that they were required to pass through the sodium beam. This care enabled the molecular beam useful to the basic experiment to be determined from the measured pressure change in chamber three (Sec. IIA, above).

B. Molecular Beam Source

The molecular furnace consisted of a sheet of tungsten (2 in. x 3 in. x .001 in.) which was rolled to form a cylinder (2 in. long and 3/16 in. diameter). The hole of $\tilde{\sim}$ 1 mm diameter was sandblasted in the wall of the cylinder to permit the molecular gas to escape from the furnace as a beam. Each end of the tubular furnace was closed off with molybdenum end pieces, one piece also serving as an inlet for gas molecules. This assembly was supported at the ends by two copper bus bars which conducted

the ac current (up to 300 amps) for Joule heating of the furnace. The molecular gases introduced into this furnace in the course of experimentation were 99.9% pure.

The furnace geometry required that each molecule make an average of approximately 10^3 collisions with the walls before escaping into the beam, and the use of tungsten wire wadding inside the furnace further increased contact of the gas with the hot furnace surfaces. The kinetic temperature of the beam molecules was checked as a function of furnace pressure in a separate experiment, using a high resolution seven-disc rotating velocity analyzer and a mass spectrometric detector. The results of these measurements verified that kinetic equilibrium was reached by the gas in the furnace and that for pressures up to 4 Torr (the highest used in the experiments) expansion of the gas into the vacuum did not cause significant deviations from the Maxwell-Boltzmann distribution.

The furnace temperatures for N_2 ranged from 2000 to 3000°K; those for H_2 and D_2 ranged from 2000 to 2600°K. At these temperatures, the excitation of any molecular electronic state is negligible. (The first electronic states of H_2 and N_2 are more than 10 eV and 6 eV above the ground state respectively). The temperature range for the hydrogen isotopes is more limited because their dissociation becomes very significant at temperatures approaching 2600°K. The excitation signals using H_2 and D_2 had to be corrected for the decrease in molecular number density at the higher experimental temperature so that the correct excitation rate constants would be determined.

The furnace temperature was measured with an optical pyrometer

while the molecular gases were being admitted. The pyrometer was made to view the inside of the furnace aperture.

The molecular number density in the interaction region (without velocity selection) was of the order of 10^{12} cm^{-3} throughout these experiments.

C. Atomic Beam Source

The sodium beam source was a two-chamber oven of conventional design machined from blocks of Monel metal. Sodium metal was placed in the rear chamber where it was vaporized at about 550°K. The vapor was free to pass through a short stainless steel tube into the front chamber where the temperature was 650°K. The number density of this beam in the interaction region was approximately 1×10^{10} cm^{-3}.

At this density the beam was not optically thin for radiation scattered toward the photon detector. The Doppler width due to the component of relative atom motion in the direction of the detector, for our geometry, leads to estimating the effective Doppler cross section at peak to have a value of the order of 10^{-10} cm^2. Since the maximum photon path length in the interaction region was about 1 cm, some radiation could be trapped within the beam and be re-emitted isotropically. This effect would render the already good assumption of isotropically emitted radiation[11] even better.

A second effect of not having an ideal optically thin sodium beam is that the source of detected photons would tend to be toward the side of the beam nearest the furnace when resonantly scattered photons are detected, while the source of collision-produced photons will extend

uniformly across the sodium beam. However, the magnitude of the optical thickness does not appear to require correcting for this effect.

D. Absorption Cell

The role of this device in the basic experimental configuration has been described in Section II. The basic construction corresponded to that of the sodium beam source. Two holes were drilled through opposite sides of the front chamber to allow the molecular beam to pass cleanly through. Sodium metal was placed in the other chamber. Both chambers were heated to 470°K. Vapor effused from the rear to the front chamber, where it was free to intercept the resonant furnace photons passing through.

Sodium vapor escaped from the absorption cell through the molecular beam entrance and exit holes, and unquestionably some of this sodium reached the region viewed by the photon detector. Its presence did not affect the experiment however since photons from this sodium, produced either by fluorescence or collisions, could produce only dc signals which were eliminated in the detection circuitry.

E. Velocity Selectors

Two neutral particle multi-slotted-disc velocity selectors were developed and used for the present experiments. The first was an analyzer to study the distribution of velocities issuing from the beam sources. This instrument was a dual-range velocity analyzer[12], with seven slotted discs, located in order to give no velocity sidebands. Its resolutions (full width at half maximum) were calculated to be 13.3%

in the forward direction and 3.5% in the reverse direction.

The second instrument was used as a velocity selector for the molecular beam in the excitation experiments. Since overall length was of importance, this selector had only three discs, and gave an approximately triangular pass band whose width (full width at half maximum) was calculated to be 26% of the nominal velocity, V_o. The selector admitted the odd-numbered subharmonic velocities of V_o, i.e., V_o/n, $n = 3, 5, \ldots$, with transmission falling off as $1/n$. The maximum value of V_o was limited by mechanical stability to 4.4×10^5 cm/sec. The calculated properties of the velocity selector were confirmed using the velocity analyzer.

IV. EXPERIMENTAL PROCEDURE

A. Basic Configuration

The tungsten furnace and cross beam sodium oven temperatures were set and permitted to stabilize. The molecular gas pressure in the source was brought to its operating level, $\tilde{\sim}$ 4 Torr, and the furnace temperature was measured using the optical pyrometer looking into the furnace aperture. The resonantly scattered furnace light signal was noted.

The molecular gas was turned off. The absorption cell was heated to its temperature, resulting in a drop of the scattered light signal. The tungsten furnace temperature was adjusted between the highest and lowest values at which data were recorded in order to be assured that the signal observed with the beam off gave a common signal zero. Gas was then admitted to the furnace and the signal rise due to reaction was noted for the particular furnace temperature. Following observation of the signal, the gas was turned off and the pressure change in the experimental vacuum chamber was noted in order to calculate n_1.

These observations provide sufficient data to determine the excitation rate constant at all temperatures for N_2. In the cases of H_2 and D_2, an additional procedure was appended, since here the flux of molecules leaving the furnace is not constant with temperature as was the verified situation for nitrogen. The hydrogen molecular beam fluxes are temperature dependent because of thermal dissociation. It became necessary to measure the dissociation fraction at each temperature for these molecules so that number densities at which dissociation occurs could be inferred using the number densities at which dissociation does not occur.

For this purpose, the molecular beam was chopped and a quadrupole mass spectrometer (Extranuclear Laboratories Model 324-9) coaxial with the molecular beam was activated. The mass spectrometer signals, proportional to number density, for masses two and four, when the gas admitted to the furnace was H_2 and D_2 respectively, were recorded as a function of temperature between 1800 and 2800°K (holding the total gas flow rate constant). Since there was essentially no dissociation of these species at 2000°K, the pressure rise in chamber three due to the molecular beam being turned on gives the correct molecular number density at that temperature. With knowledge of the spectrometer signals at various temperatures relative to the signal at 2000°K, the rate constants at the other temperatures could be determined. Other specific details are discussed with the data in Section V.

Due to the fact that H_2 and D_2 dissociate significantly near 2600°K at furnace pressures of several Torr, it was necessary to verify that the excitation signals were, in fact, not due to the conversion of relative kinetic energy and electronic energy via atom-atom collisions. To this end, the tungsten furnace temperature was held constant and the molecular pressure inside the furnace was increased. Since the dissociation fraction, i.e., relative amounts of H and H_2, can be made to vary substantially by this exercise, observation of the change in excitation signals with change in dissociation fraction is a test for the predominance of either an atomic or molecular excitation mechanism. During this test while the temperature was 2800°K and the molecular pressure was reduced so that the predominant beam component was atomic hydrogen no excitation signals were observed. When the furnace pressures

were high (molecular hydrogen predominance), the excitation signals increased proportionally as the molecular number density. Since the signals followed the changes in molecular number density and not those of the atomic constituent, the measured signals are clearly due to only hydrogen molecules.

An additional test was performed concerning the observability of an atom-atom excitation mechanism using beam intensities comparable to those used for atom-molecule excitation. In this test, only Helium or Argon gas was introduced into the molecular furnace and no excitation signals were observed.

B. Velocity-Selected Configuration

The primary beam velocity selector was first calibrated using the velocity analyzer, followed by mass spectrometric detection and using a modulated beam from the molecular beam source. The dual range calibration method[11] was performed at room temperature and checked at 2600°K for nitrogen. The velocity selector was kept in its calibrated in-beam position throughout experimental runs. With the tungsten furnace and the sodium source temperature stabilized, the velocity selector was set for a particular rotational speed and the change in the phase-sensitive scattered light signal was measured when gas was admitted to the molecular furnace. After every two or three points taken at different rotational speeds, the selector was brought back to an arbitrary reference speed for the purpose of verifying constancy of the experimental conditions throughout the time period required to gather these data. For nitrogen, velocity contours were taken at 2600 and 2900°K; for hydrogen and deuter-

ium, 2600°K was the only molecular beam temperature.

The above-described procedure produced curves of signal *vs.* selector speed, with the signal being given in arbitrary units. In order to normalize these curves with respect to each other, a separate measurement was performed. With the selector speed chosen such that signals could be observed from the three gases, N_2, H_2 and D_2, each of these gases was successively admitted under fixed flow conditions and the photon signals were observed. The velocity selector was then lowered out of the beam and the relative number densities for the respective beams were determined using the mass spectrometric procedures used in the basic configuration experiments. From these data it was straightforward to obtain a single arbitrary unit scale for the signals from the three molecular species used in the experiments.

V. RESULTS

The temperature-dependent effective rate constants determined with the basic configuration for H_2, D_2 and N_2 are shown in Fig. 2. The ordinate, η, is defined by Eq. (12).

The excitation rate for N_2 was determined absolutely at 2200°K using the procedure of comparing reactive signals with resonantly scattered furnace light signals as described in Sections II and IV above. The absolute rates for H_2 and D_2 were determined by comparing the reactive signals for these gases with the N_2 signal at 2200°K. These determinations carry the assumptions that (a) the ionization gauge relative efficiency factors are known (N_2 is more efficiently detected than H_2 and D_2 by a factor of 2.4), and (b) the diffusion pumping speeds for H_2 and D_2 relative to N_2 are related by the inverse square root of the mass ratios.

The rate constants at temperatures other than 2200°K were determined for each gas from relative measurements of that gas with respect to 2200°K. All quoted error bars in Fig. 2 refer solely to the reproducibility of data at each point; their magnitude corresponds to the mean deviation of the average signals.

The velocity-selected signals obtained for H_2 and D_2 at 2600°K are displayed in Fig. 3; those for N_2 at 2600 and 2900°K are shown in Fig. 4. The abscissa, V_o, is the nominal laboratory speed of the velocity-selected molecules prior to excitation collisions. The data of both figures are plotted using the same arbitrary units for signal. The respective signals were adjusted to the same scales as a result of taking relative velocity measurements at $V_o = 3 \times 10^5$ cm/sec and measuring the relative molecular beam densities without velocity selection. Similarly, as in the

basic configuration, the relative scaling is known only to within the same relative pressure gauge efficiency factors and diffusion pumping speeds.

VI. DISCUSSION OF RESULTS

Figures 3 and 4 show direct data taken in the experiment, and represent signals that are integrated over both internal energy and the kinetic energies of both beams. Even with the absolute rate coefficient data given in Fig. 2, these data are insufficient to determine the cross section as a function of relative velocity or kinetic energy for each internally excited state.

It is possible, however, to assume reasonable velocity dependences of the cross sections, leaving their absolute values as parameters, then predict signals and finally assign the parameters by comparison with the actual experimental results. In this section such a procedure is followed using two different energy dependences.

A. N_2 + Na

Theory indicates[13,14] that the most important form of molecular internal energy for processes of the type under study is vibrational energy, and it is here assumed that only vibrational energy need be considered. It is further assumed that the cross section as a function of velocity, w, for a given vibrational state is either of two forms:

$$\sigma_r(v,v';w) = \sigma_{v,v'} R_{\Delta v}^{(a)}, \text{ where } R_{\Delta v}^{(a)} = \begin{cases} 0 & w < w_t \\ 1 & w > w_t \end{cases} \qquad (14a)$$

or

$$\sigma_r(v,v';w) = \sigma_{v,v'} R_{\Delta v}^{(b)}, \text{ where } R_{\Delta v}^{(b)} = \begin{cases} 0 & w < w_t \\ 1 - (w_t/w)^2 & w > w_t \end{cases} \qquad (14b)$$

where v and v' are the initial and final vibrational quantum numbers, $\sigma_{v,v'}$ are constants, w_t is the threshold velocity given by

$$w_t = \sqrt{\frac{2}{\mu}\left[E_o - (\varepsilon_v - \varepsilon_{v'})\right]} \tag{15}$$

where μ is the reduced mass and ε_v ($\tilde{=} v\hbar\omega_o$) is the energy of the v-th vibrational state. Eq. (14a) describes a step-function kinetic energy dependence and Eq. (14b) describes an energy dependence which is a step function of the kinetic energy component along the line of centers between two particles undergoing a hard-sphere collision.

By limiting the form of internal energy to vibrational energy only, Eqs. (9), (11) and (12) can be re-written for the basic configuration experiment as

$$\eta(T_1) = \sum_v \sum_{v'} \sigma_{v,v'}\, p_{v,v'}(T_1) \tag{16}$$

where

$$p_{v,v'}(T_1) = e^{E_o/kT_1}\left[P_{\Delta v}(T_1)\,\frac{e^{-\varepsilon_v/kT_1}}{\sum_v e^{-\varepsilon_v/kT_1}}\right] \tag{17}$$

and

$$P_{\Delta v}(T_1) = \int_o^\infty du_1 \int_o^\infty du_2\, w\, R_{\Delta v}(w)\, f(u_1)f(u_2)$$

$$= \frac{2(\alpha_1\alpha_2)^{3/2}}{\delta} \int_{w_t}^\infty R_{\Delta v}(w)\, w^4 I_1(\delta w^2) e^{-\gamma w^2}\, dw \tag{18}$$

where $R_{\Delta v}$ is defined by either of Eqs. (14a) and (14b).

In the velocity-selected configuration experiment, referring to Eqs. (4) and (13), the signals are given by

$$S(V_o,T_1) = Ck_r' = C\sum_{vv'} \sigma_{v,v'} q_{v,v'}(V_o,T_1) \tag{19}$$

where the apparatus constant, C, is defined in Eq. (14),

$$q_{v,v'}(V_o,T_1) = Q_{\Delta v}(V_o,T_1) \frac{e^{-\varepsilon_v/kT_1}}{\sum_v e^{-\varepsilon_v/kT_1}} \tag{20}$$

and

$$Q_{\Delta v}(V_o,T_1) = \int_o^\infty du_1 \int_o^\infty du_2 R_{\Delta v}(w) wB(V_o,u_1) f(u_1) f(u_2). \tag{21}$$

The quantity $Q_{\Delta v}(V_o,T_1)$ is readily calculable and is shown for the case of N_2 + Na at $T_1 = 2900^oK$ in Figs. 5(a) and 5(b) for the two forms of $R_{\Delta v}$. For $\Delta v \leq 5$, $Q_{\Delta v}$ is too small to be plotted in the figures. The "experimental" curve is a smooth curve drawn through the experimental points of Fig. 4 and is shown for reference only. Since each curve for a given Δv depicts the shape of the signal expected, had the signal arisen only from transitions with that Δv, it is obvious that in the velocity-selected experiment, the observed signals were weighted superpositions of signals from transitions with all Δv's present, and that substantial fractions of the signals arose from transitions in which kinetic energy took part.

A set of weighting coefficients, $h_{\Delta v}(T_1)$, can be found by fitting the experimental results to

$$S(V_o,T_1) = \sum_{\Delta v} h_{\Delta v}(T_1) Q_{\Delta v}(V_o,T_1) \tag{22}$$

The physical significance of the weighting coefficients is evident upon re-writing Eqs. (19) and (20) in the form

$$S(V_o,T_1) = C \sum_{\Delta v} g_{\Delta v}(T_1) Q_{\Delta v}(V_o,T_1) \tag{23}$$

$$g_{\Delta v}(T_1) = \sum_{v} \sigma_{v,v-\Delta v} \frac{e^{-\varepsilon_v/kT_1}}{\sum_{v} e^{-\varepsilon_v/kT_1}} \tag{24}$$

i.e., $h_{\Delta v}(T_1)$ differs from the physically significant $g_{\Delta v}(T_1)$ by the multiplying apparatus constant, C, of the velocity-selected experiment.

The absolute value of the constant C can be determined using the data of the basic configuration experiment, as can be seen from re-writing Eqs. (16) and (17)

$$\eta(T_1) = \sum_{\Delta v} P_{\Delta v}(T_1) e^{E_o/kT_1} g_{\Delta v}(T_1) \tag{25}$$

from which

$$C = \frac{\sum_{\Delta v} P_{\Delta v}(T_1) e^{E_o/kT_1} h_{\Delta v}(T_1)}{\eta(T_1)} \tag{26}$$

The absolute value of the physical quantity, $g_{\Delta v}(T_1)$ is then given by

$$g_{\Delta v}(T_1) = \eta(T_1) \frac{h_{\Delta v}(T_1)}{\sum_{\Delta v} P_{\Delta v}(T_1) e^{E_o/kT_1} h_{\Delta v}(T_1)} \tag{27}$$

The ultimate knowledge desired is the set of values of the cross section parameters, $\sigma_{v,v'}$. If the experimental data were sufficiently precise these could be obtained by determining $g_{\Delta v}(T_1)$ at many temperatures and then solving the simultaneous equations, Eqs. (24). Unfortunately, the data were not sufficiently precise and the temperature range was too small

to warrant carrying out the entire procedure. However, it is instructive to consider the evaluation of $g_{\Delta v}(T_1)$ at $T_1 = 2600^{\circ}K$, in the middle of the experimental temperature range, and several consequences.

Table 1 gives the values of $g_{\Delta v}(2600)$ using both forms of $R_{\Delta v}$, obtained through the use of Eq. (27). In constructing this table, all transitions with $\Delta v > 8$ are neglected, i.e., all transitions requiring no kinetic energy are ascribed to $\Delta v = 8$, the effect of which is to overestimate the true $\Delta v = 8$ transitions effects.

Table 2 uses the values of Table 1 and presents the sums of cross sections specified by Eq. (24). The first line in Table 2 is of interest. It indicates that if the kinetic energy dependence of transfer is a step-function, i.e., $R_{\Delta v}^{(a)}$ is used, then an upper limit for the 8-0 transition is far below what would be required to make the Hunten hypothesis on excitation of atmospheric sodium attractive.

If other kinetic energy dependences are obtained, this conclusion cannot be drawn as firmly, and an energy dependence given by $R_{\Delta v}^{(b)}$ could indeed place $\sigma_{8,0}$ in the range required by Hunten, if other $\Delta v = 8$ transitions are not significant in the experiment, a point which could not be clarified by the data of these experiments. Hooymayers and Alkemade[15] have noted, however, that quenching cross sections appear to increase with diminishing resonance energy defect, at least for different diatomic molecules. If this observation also applies to energy defects for different vibrational energy state transitions (due to anharmonicity) in the same molecule, then it is unlikely that $\sigma_{8,0}$ is the major contributor to the sum in Table 2, in which case even with $R_{\Delta v}^{(b)}$, $\sigma_{8,0}$ would be smaller than required for the Hunten hypothesis.

It is also interesting to consider the relative contributions to the overall rate coefficient, η, by the various transitions with different values of Δv. Table 3 presents the separate terms in the sum given in Eq. (25).

It is evident from this table that in these crossed beam experiments, over half of the signals in the basic configuration came from transitions with $\Delta v = 7$. It is clear that the temperature dependence of η must therefore be governed to a very large extend by the temperature dependence of g_7, and it is evident from inspection of Eq. (24) that this requires that most of the contribution to g_7 must come from a term other than the lead term in the series. Fitting of the data, in fact, requires that the major contribution to g_7 must come from the 10-3 transition, for both forms of $R_{\Delta v}$ used in the model.

An additional exercise performed started with the assumption (1) that only one term in each series expression for the $g_{\Delta v}$'s was important and that all others could be neglected. It was further assumed (2) that each $g_{\Delta v}$ separately had the temperature dependence required to make its contribution to η and have the observed temperature dependence of η as determined in the basic configuration experiment. This is a sufficient condition for consistency of all data taken in the experiments. For the $\Delta v = 6$ and 7 transitions, the second assumption would also be a necessary condition because of the large contributions of these transitions to the experimental results.

Table 4 presents these "most probable" transitions and their corresponding cross sections. The cross section values would decrease, where the first assumption weakened.

Under the two above assumptions, the 11-3 transition is the "most probable" $\Delta v = 8$ transition. It is interesting to note that of all the $\Delta v = 8$ transitions, the 11-3 transition is most nearly resonant with the sodium excitation energy.

A test of the consistency of the analysis model with these two simplifying assumptions is shown in Fig. 6. The cross sections of Table 4, which were evaluated at 2600°K, were reinserted into the formulas (19-21) in order to predict the results of the velocity-selected experiments at 2900°K. Although the temperature difference used here is smaller than would be desired, it is seen that quite good predictions can be made at temperatures other than the one from which the cross section values were obtained.

B. Detailed Balancing Considerations

A final consideration is that of detailed balancing and a comparison with experiments on quenching of sodium D-line radiation by N_2. Extensive measurements on quenching have been made, both near room temperature[16-18] and at elevated temperatures in both flames[15,19] and shock tubes.[20]

Detailed balancing relates the excitation cross section, $\sigma_r(v,v';E)$ to the quenching cross section, $\sigma_q(v',v;E')$. The excitation cross section is defined by Eq. (14), except that here it is convenient to replace the relative velocity, w, by the kinetic energy, E, measured in center-of-mass coordinates. The parameter E' is defined in such a way as to conserve energy, i.e.,

$$E' = E - [E_o - (\varepsilon_v - \varepsilon_{v'})] = E + E_t \qquad (28)$$

Assuming that in the excitation the $^2P_{1/2}$ and $^2P_{3/2}$ states are populated according to their statistical weights, detailed balancing requires

$$\sigma_q(v',v;E') = \frac{E}{3(E-E_t)}\,\sigma_r(v,v';E) = \frac{E'+E_t}{3E'}\,\sigma_r(v,v';E) \qquad (29)$$

Since most experiments have used either room temperature gases or flames operating at up to about 2000°K, principal interest attends the case for which $v' = 0$.

If $R^{(b)}_{\Delta v}$ is used to describe the kinetic energy dependence for the excitation cross sections, then substitution of Eq. (14b) into the first form of Eq. (29) gives a quenching cross section that is independent of kinetic energy, E', and

$$\sigma_q(0,v;E') = \sigma_{v,0}/3 \qquad (30)$$

Referring to Table 2, the tabulated values in Column IV are upper limits on the cross sections $\sigma_{v,0}$, and hence applying Eq. (30) to these tabulated values should give an upper limit on the cross section for quenching sodium resonance radiation, in which the N_2 ends up in states with $v \geq 4$. The upper limit so obtained is about $50(\pm 20) \times 10^{-16}$ cm^2. This is very close to values measured[15,16] near room temperature ($\sim 40 \times 10^{-16}$ cm^2). Since the velocity-selected data indicate that at least for the $\Delta v = 6$ and 7 transitions the 6-0 and 7-0 transitions are not the major terms in the sums of Table 2, it must be concluded that quenching in which the N_2 ends up in states with $v \leq 3$ is quite probable, if the kinetic energy dependence of the excitation cross section is that given by $R^{(b)}_{\Delta v}$.

If $R^{(a)}_{\Delta v}$ is used, the quenching cross section has an energy dependence of the form $(1 + E_t/T')$. Upon integration over a Maxwell-

Boltzmann velocity distribution the rate coefficient for quenching is

$$k_q = \int \sigma_q(u) u f(u) du = \frac{\sigma_{v,v'}}{3} \bar{u}(1 + E_t/kT) \qquad (31)$$

where $f(u)$ and $\sigma_{v,v'}$ are defined in Eqs. (10) and (14a) respectively and $\bar{u} = (8kT/\pi\mu)^{1/2}$. It is common in quenching experiments to measure the rate coefficient, k_q, and then divide by $\bar{u}$ in order to obtain an "effective cross section", $S(T)$. On the assumption that $R_{\Delta v}^{(a)}$ describes the kinetic energy dependence of the excitation cross section, the effective cross section is

$$S_{v,v'}(T) = \frac{1}{3} \sigma_{v,v'}(1 + E_t/kT). \qquad (32)$$

Effective quenching cross sections measured at room temperature and at flame temperatures are of comparable magnitude and do not display the strong temperature dependence called for by Eq. (32). Evidently $R_{\Delta v}^{(a)}$ is not as good as $R_{\Delta v}^{(b)}$ in describing the excitation cross section's energy dependence. On the other hand, Hooymayers and Alkemade[15] found that in flames working over the temperature range 1700-2500°K, the effective cross section appeared to vary inversely with the temperature, which suggests the opposite conclusion. Since in the flame experiments quenching by excited N_2 as well as groundstate N_2 can occur, it appears possible that kinetic energy dependences of excitation cross sections, for different vibrational transitions may be more complicated than assumed in the present analysis.

Comparison with Theory

Two theoretical studies of the quenching of Na^* by N_2 have been carried out. Both treated the problem as involving the formation of an ionic complex, $Na^+ \cdot N_2^-$, in which multiple crossings of potential curves occurs, followed by dissociation into groundstate Na and $N_2(v)$. Both calculations considered quenching by only groundstate N_2. Whereas Bjerre and Nikitin[13] calculated a quenching rate coefficient at 1000°K from which effective cross sections can be derived, Bauer, Fischer and Gilmore[14] pointed out that with the strong coulomb attraction between the Na^+ and N_2^- components, acceleration would make unimportant any kinetic energy (up to 0.5 eV) of the particles prior to complex formation, and calculated energy-independent cross sections directly. Details of the calculations differed and somewhat different results were obtained.

The approach used by Bjerre and Nikitin led to predicting that, whereas all vibrational states would be populated in quenching, the peak of the vibrational population would occur at v = 2, and that quenching to the v = 1, 2 and 3 states would account for about 95% of the total quenching cross section.

The approach of Bauer, Fischer and Gilmore led to broader predicted distributions of population across the vibrational states, the actual distribution and the total cross section depending on the assumed value of the sum of the polarizabilities of Na^+ and N_2^-. For an assumed polarizability sum of 10 A^3, the total cross section was in good agreement with that of Bjerre and Nikitin and also with experiment; the distribution peaked at v = 5, with contributions from v = 4, 5 and 6 giving about 80% of the total cross section.

The temperature independence of the quenching cross section pointed out by Bauer et al[14] implies through detailed balancing that for the excitation cross section the kinetic energy dependence should be that given by $R^{(b)}_{\Delta v}$, and Table 5 gives the values of $\sigma_{v,0}$ deduced from the two calculations. The table also shows the values of the cross section sums from Table 2, which are upper limits on $\sigma_{v,0}$. The general pattern of values appears to indicate that the results of Bauer et al are more compatible with the present experiments than are the results of Bjerre and Nikitin.

B. Na + H_2 and Na + D_2

Because of the larger energy spacings in the hydrogen molecules, the Na D-line radiation can be excited from the v = 5 state of H_2 and from the v = 7 state of D_2, with excess energies of approximately 0.19 eV in both cases. Proceeding analogously to the case of N_2 excitation, the quantities $Q_{\Delta v}(V_o,T_1)$ were superposed to fit the velocity-selected data shown in Fig. 3, and it was believed that for H_2, the $\Delta v = 4$ and 5 and for D_2 the $\Delta v = 5$, 6, and 7 could be identified. From the weighting factors found, the values of $\eta_{\Delta v}/\eta$ suggested that under the conditions of the experiment, for H_2 the $\Delta v = 4$ and 5 transitions participate about equally in signal production, and the temperature dependence of η in the basic experiment favors these transitions being the $5 \rightarrow 0$ and $4 \rightarrow 0$ transitions. In the case of D_2, the $6 \rightarrow 0$ transition appeared to be the most important one for signal production in the present experiments.

A serious difficulty in working with H_2 and D_2 in the present experiments lay in the fact that the velocity selector maximum speed

($V_o = 4.4 \times 10^5$ cm/sec) was not sufficiently high to allow the observation of any Δv transitions other than those indicated in the above paragraph. Additionally, because at the highest velocity selector speeds, the kinetic energy effects were just beginning to become evident, the uncertainties in selecting the weighting factors, $h_{\Delta v}$, are much greater in the case of H_2 and D_2 than for N_2. The inability to observe transitions in which substantial kinetic energy is present in the velocity-selected experiments precludes attempting to analyze the hydrogen results in the detail applied to the N_2 results. No further discussion of the H_2 and D_2 results appears to be warranted.

VI. ADDED NOTE ON A SIMILAR EXPERIMENT

Following conclusion of the experimental work contained herein, the authors received copies of the doctoral thesis of P. J. Kalff at the University of Utrecht which reported on similar crossed beam experiments on excitation transfer between heated N_2 and both Na and K atoms.[21] Kalff's general approach was similar to that of Mentall, Krause and Fite[9] and to that used in the "basic configuration" experiments described herein, but had two significant differences: First, the experiment was a dc experiment rather than a modulated beam experiment, and thus may have been subject to certain stray light problems that the modulation techniques preclude, and, second, rather than using a total calibration procedure based on the black body radiation from the molecular beam source, Dr. Kalff elected to measure separately the beam intensities, collision and detector geometries, and either to measure or use manufacturers' calibrations for other experimental parameters (filter transmission, photomultiplier quantum efficiency and gain, etc.) required for a step-wise calibration of the entire experiment.

The results of the two experiments on the excitation of Na by N_2 show very good agreement on the temperature dependence of the reaction rate coefficient (Fig. 2). However, in absolute magnitude Kalff's results were lower than those presented here by about a factor of 3.

It is the opinion of the present authors that the values indicated in Fig. 2 are to be preferred. It appears difficult to achieve consistency between the velocity-selected experimental data of the present experiments, the known inverse quenching rate coefficients and the

excitation rate coefficient quoted by Kalff. Additionally, it is noted that the step-wise calibration procedure used by Kalff admits the possibility of more serious cummulative errors than the calibration method used in the present experiments.

REFERENCES

1. D. R. Jenkins, Proc. Roy. Soc., A293, 493 (1966).
2. J. C. Polanyi, J. Quant. Spectry. Rad. Transfer 3, 471 (1963).
3. J. G. Clouston, A. G. Gaydon, and I. I. Glass, Proc. Roy. Soc. (London) A248, 429 (1958).
4. A. G. Gaydon and I. R. Hurle, Symp. Combust. 8th, Pasadena, Calif. 1960, 309 (1962).
5. I. R. Hurle, J. Chem. Phys. 41, 3911 (1964).
6. W. L. Starr, J. Chem. Phys. 43, 73 (1965).
7. H. Derblom, J. Atmosph. Terr. Phys. 26, 791 (1964).
8. D. M. Hunten, J. Atmosph. Terr. Phys. 27, 583 (1965).
9. J. E. Mentall, H. F. Krause, and W. L. Fite, Disc. Faraday Soc., 44 (1967).
10. A. C. G. Mitchell and N. W. Zamansky, Resonance Radiation and Excited Atoms, Cambridge University Press.
11. J. W. Chamberlain, Physics of the Aurora and Airglow, (Academic Press, New York, 1961), p. 448.
12. Arthur E. Grosser, Rev. Sci. Instr. 38, No. 2, 257 (1967).
13. A. Bjerre and E. E. Nikitin, Chem. Phys. Letters 1, 179 (1964).
14. E. Bauer, E. R. Fischer, and F. R. Gilmore, J. Chem. Phys. 51, 4173 (1969).
15. H. P. Hooymayers and C. Th. J. Alkemade, J. Quant. Spect. Rad. Transfer 6, 847 (1966).
16. R. G. W. Norrish and W. M. Smith, Proc. Roy. Soc. A176, 295 (1941).
17. W. Demtroeder, Z. Physik 166, 42 (1962).
18. B. P. Kibble, G. Copley, and L. Krause, Phys. Rev. 159, 11 (1967).

19. D. R. Jenkins, Proc. Roy. Soc. (London) A293, 493 (1966); A303, 453 (1968).

20. S. Tsuchiya and K. Koratan: Combustion and Flame, 9, 299.

21. P. J. Kalff, "Alkaline Earth Compounds in Flames and N_2-Alkali Energy Transfer in Molecular Beams", Thesis, University of Utrecht, Drukkerij Bronder-Offset N.V., Rotterdam, (1971).

FIGURE CAPTIONS

1. Sketch of the experimental arrangement. Light baffles used to diminish stray light originating from the tungsten furnace are omitted.
2. Effective rate constant, η, for Na(3P) excitation in the basic arrangement from collisions with H_2, D_2 and N_2 at temperature, T_1.
3. Light signals for Na(3P) excitation with velocity-selected H_2 and D_2 at 2600°K.
4. Light signals for Na(3P) excitation with velocity-selected N_2 at 2600° and 2900°K.
5. Contributions $Q_{\Delta v}(V_o, T_1)$ for velocity-selected N_2 at 2900°K using (a) cross section $R_{\Delta v}^{(a)}$ and (b) cross section $R_{\Delta v}^{(b)}$.
6. Comparison of N_2 experimental data with signals from all participating states for cross sections $R_{\Delta v}^{(a)}$ and $R_{\Delta v}^{(b)}$.

Δv	$g_{\Delta v}(2600^{\circ}K)$	
	Using $R_{\Delta v}^{(a)}$	Using $R_{\Delta v}^{(b)}$
8	$(0.24 \pm 0.2) \times 10^{-20}$ cm^2	$(1.9 \pm 1) \times 10^{-20}$ cm^2
7	(9.6 ± 3)	(22 ± 5)
6	(27 ± 10)	(104 ± 30)
5	(82 ± 30)	(700 ± 300)
4	(600 ± 400)	(3500 ± 2000)
3	(2000 ± 15000)	

Table 1. Values of $g_{\Delta v}(2600^{\circ}K)$ from Eq. (27).

I	II	III	IV
		Using $R_{\Delta v}^{(a)}$	Using $R_{\Delta v}^{(b)}$
$\Delta v = 8$	$\sigma_{8,0} + 0.292\ \sigma_{9,1} + 0.085\ \sigma_{10,2} + 0.025\ \sigma_{11,3} + \ldots =$	0.6 ± 0.4 Å^2	5 ± 3 Å^2
7	$\sigma_{7,0} + 0.292\ \sigma_{8,1} + 0.085\ \sigma_{9,2} + 0.025\ \sigma_{10,3} + \ldots =$	7 ± 2	17 ± 5
6	$\sigma_{6,0} + 0.292\ \sigma_{7,1} + 0.085\ \sigma_{8,2} + 0.025\ \sigma_{9,3} + \ldots =$	4.3 ± 1.5	23 ± 7
5	$\sigma_{5,0} + 0.292\ \sigma_{6,1} + 0.085\ \sigma_{7,2} + 0.025\ \sigma_{8,3} + \ldots =$	5.3 ± 2	45 ± 20
4	$\sigma_{4,0} + 0.292\ \sigma_{5,1} + 0.085\ \sigma_{6,2} + 0.025\ \sigma_{7,3} + \ldots =$	12 ± 10	66 ± 50
3	$\sigma_{3,0} + 0.292\ \sigma_{4,1} + 0.085\ \sigma_{5,2} + 0.025\ \sigma_{6,3} + \ldots =$	12 ± 10	

Table 2. Values of Cross Section Sums

	$\eta_{\Delta v} = P_{\Delta v} g_{\Delta v} e^{E_o/kT}$			
Δv	Using $R_{\Delta v}^{(a)}$		Using $R_{\Delta v}^{(b)}$	
8	4.7×10^{-12} cm^3/sec	2%	$4.. \times 10^{-11}$ cm^3/sec	18%
7	1.2×10^{-10}	57%	1.2×10^{-10}	52%
6	5.6×10^{-11}	25%	4.2×10^{-11}	19%
5	1.8×10^{-11}	8%	1.9×10^{-11}	9%
4	1.2×10^{-11}	5%	6.6×10^{-12}	3%
3	3.2×10^{-12}	1.5%		

Table 3. Contributions of Δv transitions to η at 2600°K.

		$\sigma_{v,v'}$	
Δv	"Most Probable" Transition	Using $R_{\Delta v}^{(a)}$	Using $R_{\Delta v}^{(b)}$
8	11-3	27 $\AA^2$	190 $\AA^2$
7	10-3	300	640
6	8-2	75	290
5	6-1	20	170
4	4-0	13	78

Table 4. "Most probable" transitions for given Δv and corresponding maximum cross section values.

	Reference 13	Reference 14 ($\alpha = 10\text{Å}^3$)	Experiment (2600°)
$\sigma_{8,0}$	7×10^{-3} Å^2	0 Å^2	< 5 Å^2
$\sigma_{7,0}$	1.1×10^{-2}	6	< 17
$\sigma_{6,0}$	1.4×10^{-1}	18	< 23
$\sigma_{5,0}$	2.0	23	< 45
$\sigma_{4,0}$	4.5	18	< 66
$\sigma_{3,0}$	30	11	
$\sigma_{2,0}$	45	0.6	
$\sigma_{1,0}$	19	0	
$\sigma_{0,0}$	0	0	

Table 5. Values of $\sigma_{v,v'}$ obtained through detailed balancing from quenching cross section calculations of Refs. 13 and 14, and using $R^{(b)}_{\Delta v}$. The experimental numbers are the cross section sums from Table 2, column IV.

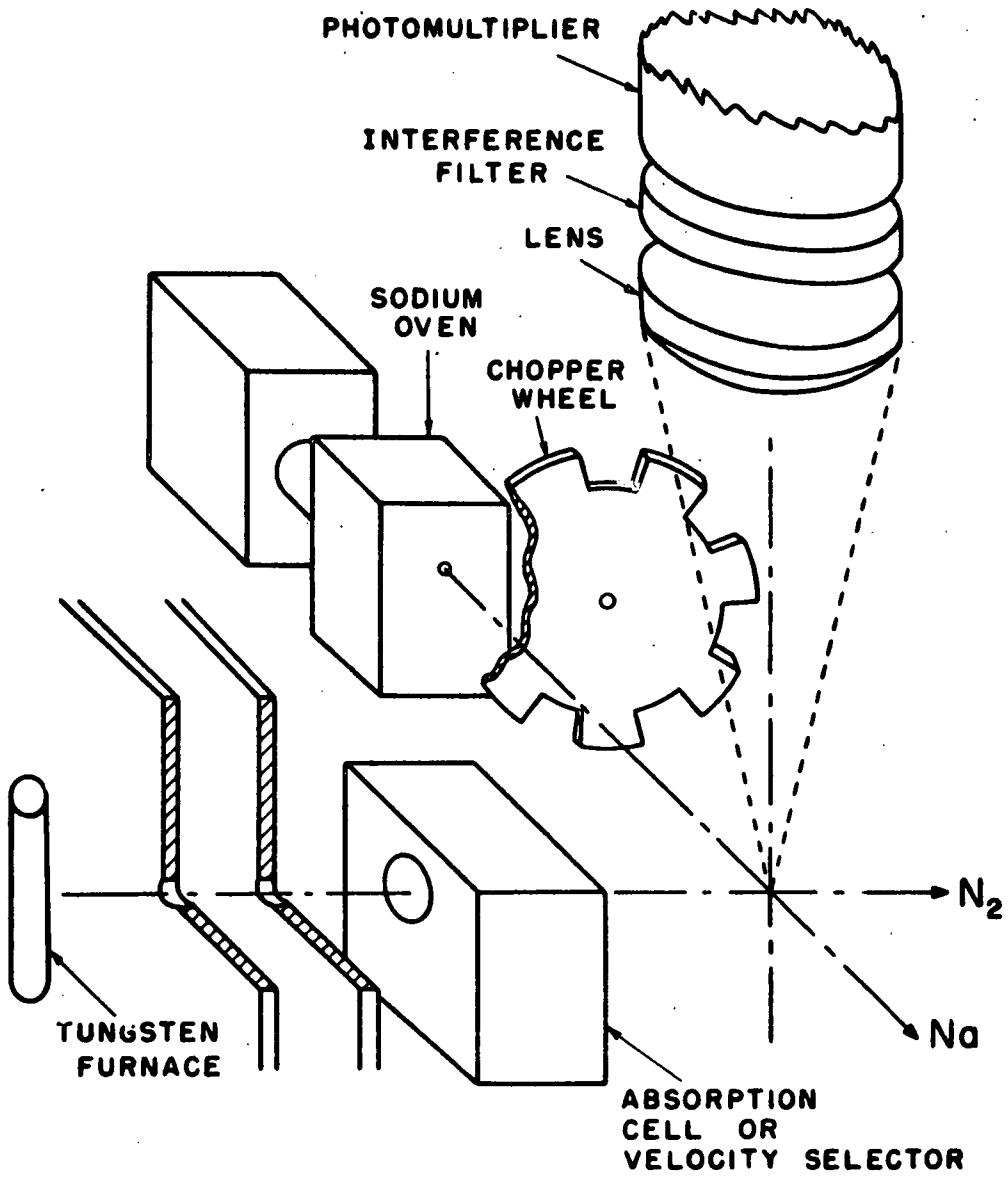
PHOTOMULTIPLIER
INTERFERENCE FILTER
LENS
SODIUM OVEN
CHOPPER WHEEL
N_2
Na
TUNGSTEN FURNACE
ABSORPTION CELL OR VELOCITY SELECTOR

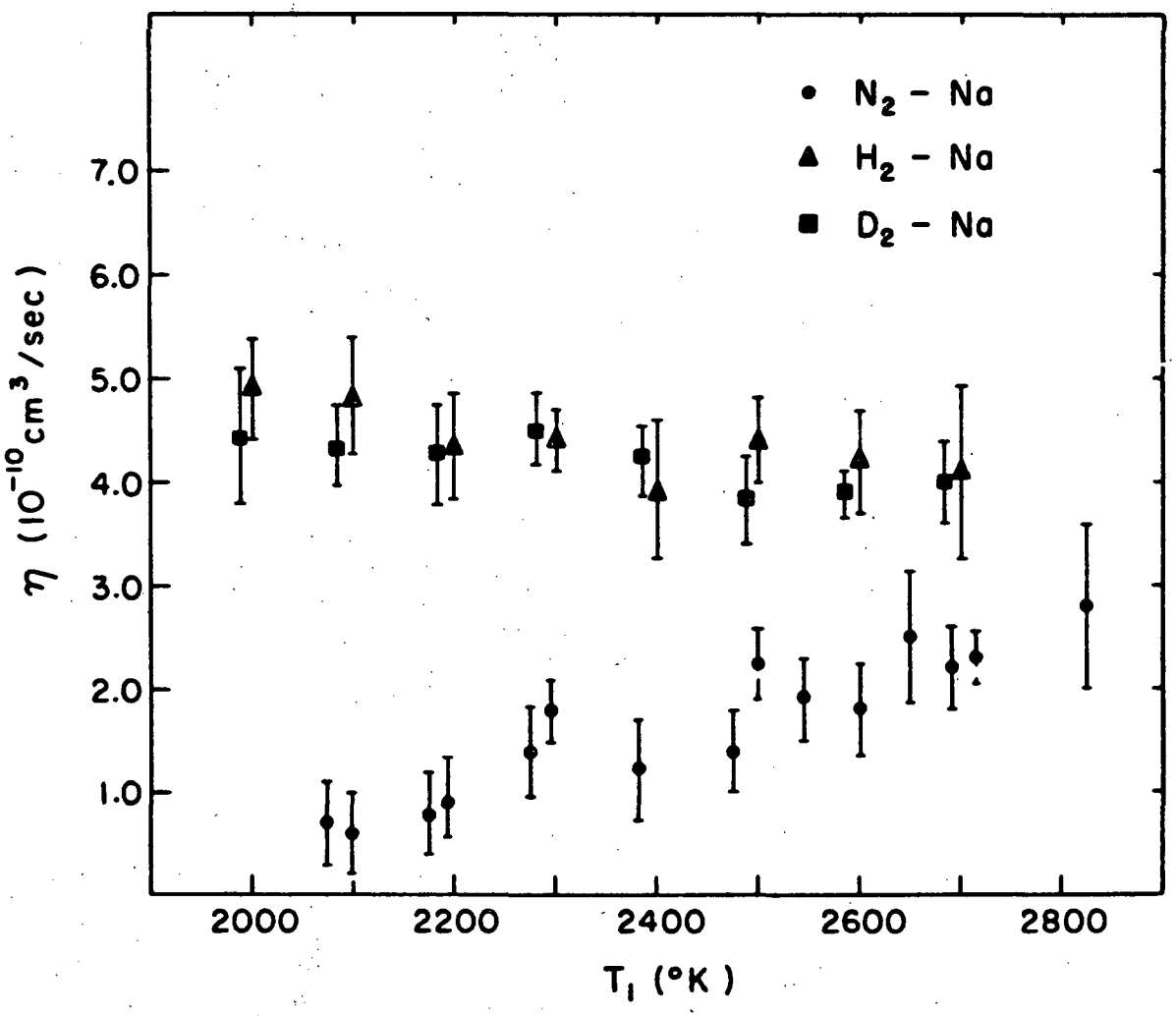
N2 - Na
H2 - Na
D2 - Na
η (10^-10 cm^3/sec)
7.0
6.0
5.0
4.0
3.0
2.0
1.0
2000
2200
2400
2600
2800
T1 (°K)

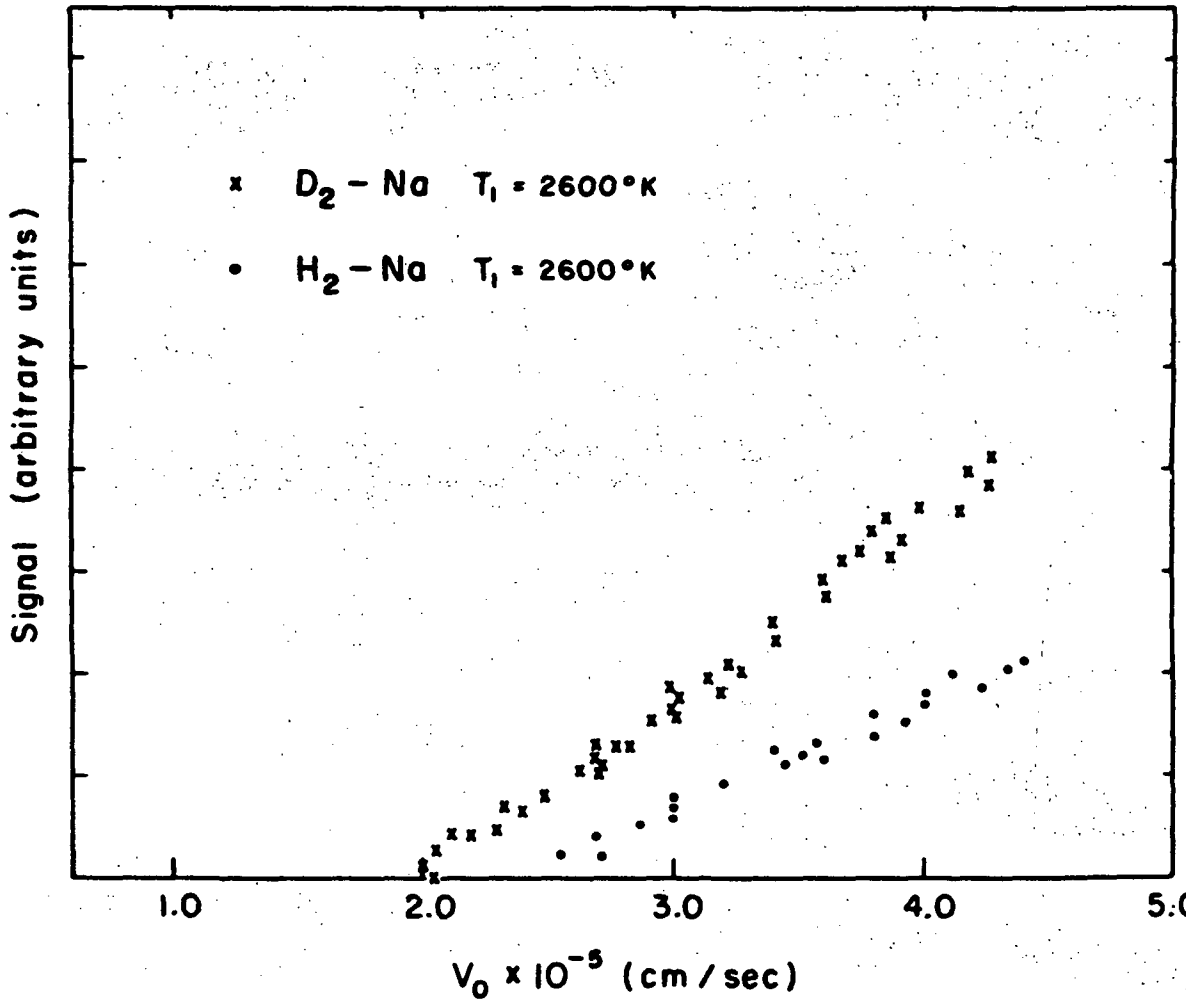
x D2 – Na T1 = 2600°K
• H2 – Na T1 = 2600°K
Signal (arbitrary units)
1.0
2.0
3.0
4.0
5.0
V0 x 10^-5 (cm / sec)

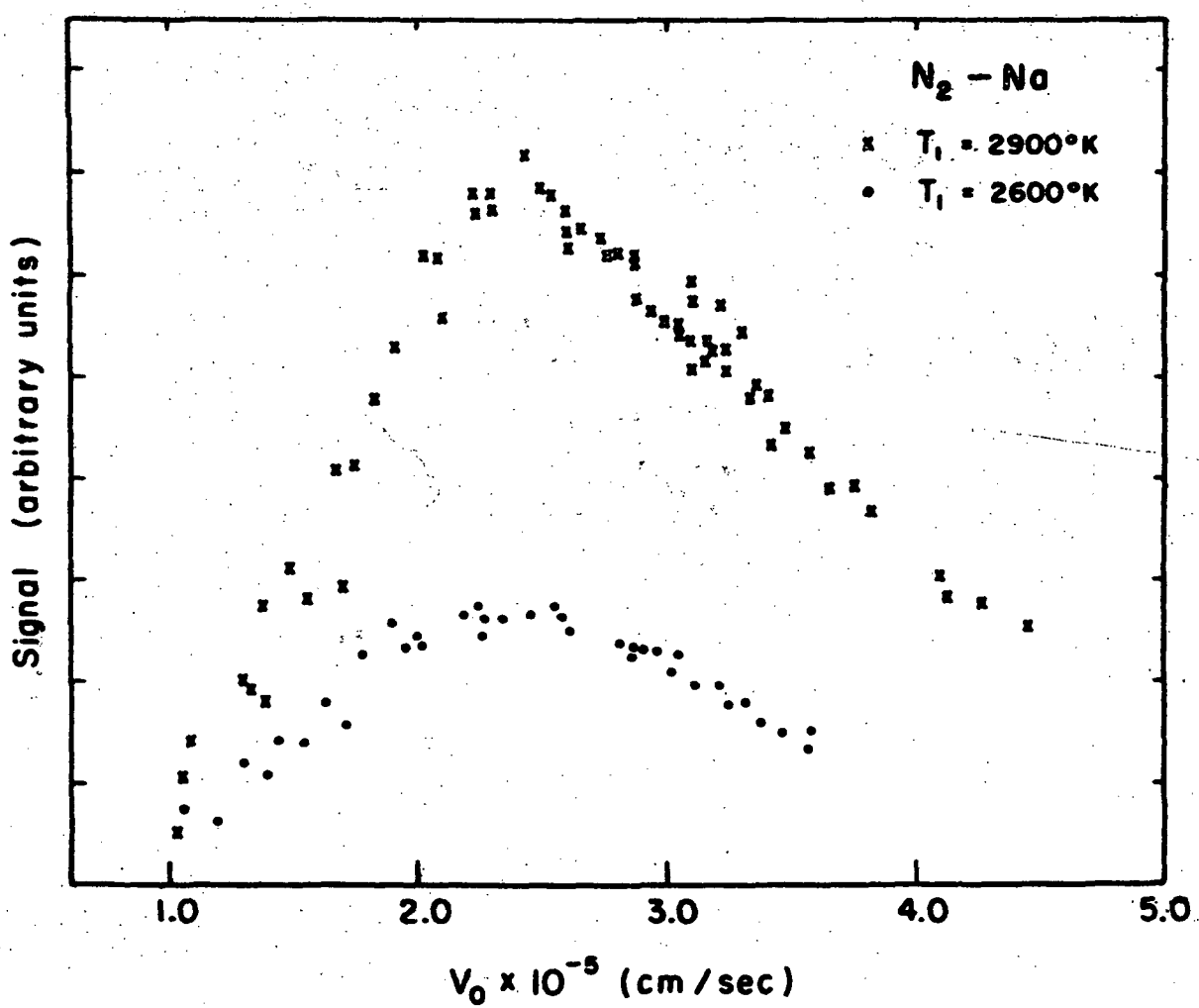
$N_2 - Na$
T_1 = 2900°K
T_1 = 2600°K
Signal (arbitrary units)
1.0
2.0
3.0
4.0
5.0
$V_0 \times 10^{-5}$ (cm / sec)

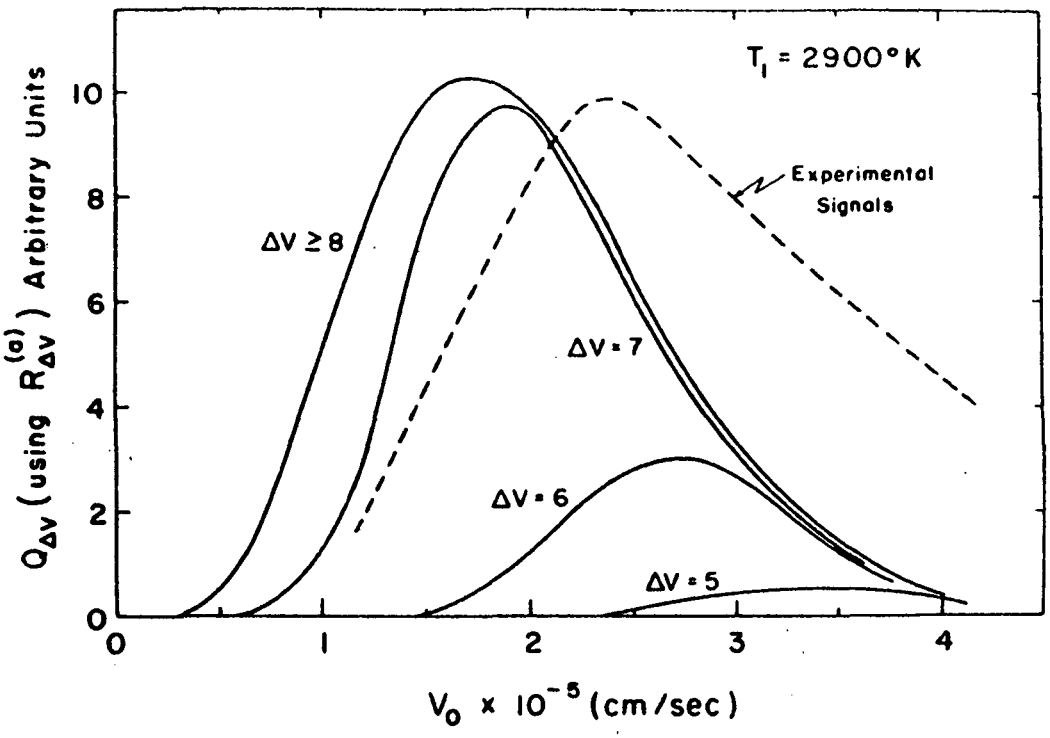
T_1 = 2900°K
Experimental Signals
ΔV ≥ 8
ΔV = 7
ΔV = 6
ΔV = 5
$Q_{\Delta V}$ (using $R^{(a)}_{\Delta V}$) Arbitrary Units
$V_0 \times 10^{-5}$ (cm/sec)
0
1
2
3
4
0
2
4
6
8
10

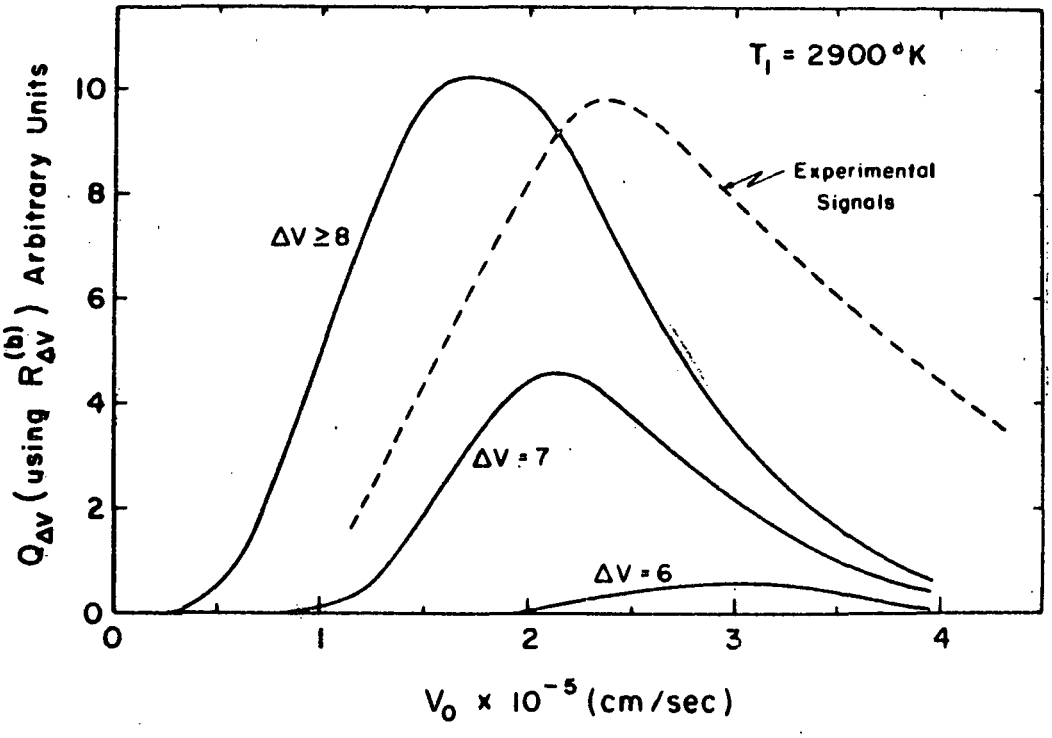
T_1 = 2900°K
Experimental Signals
ΔV ≥ 8
ΔV = 7
ΔV = 6
$Q_{\Delta V}$ (using $R^{(b)}_{\Delta V}$) Arbitrary Units
$V_0 \times 10^{-5}$ (cm/sec)
0
1
2
3
4
0
2
4
6
8
10

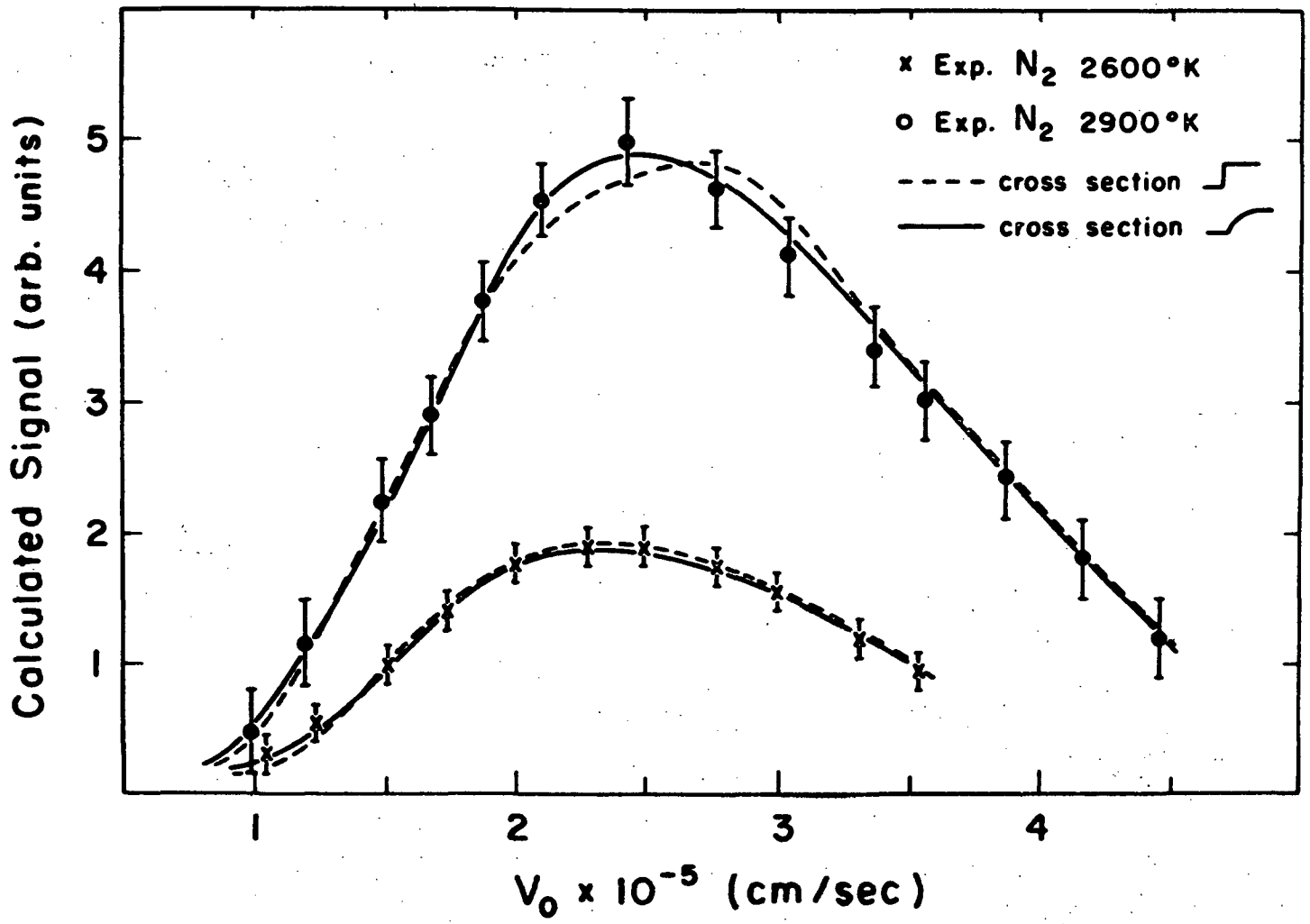
x Exp. N_2 2600°K
o Exp. N_2 2900°K
cross section
cross section
Calculated Signal (arb. units)
1
2
3
4
5
1
2
3
4
$V_0 \times 10^{-5}$ (cm/sec)